

In presenting the dissertation as a partial fulfillment of the requirements for an advanced degree from the Georgia Institute of Technology, I agree that the Library of the Institute shall make it available for inspection and circulation in accordance with its regulations governing materials of this type. I agree that permission to copy from, or to publish from, this dissertation may be granted by the professor under whose direction it was written, or, in his absence, by the Dean of the Graduate Division when such copying or publication is solely for scholarly purposes and does not involve potential financial gain. It is understood that any copying from, or publication of, this dissertation which involves potential financial gain will not be allowed without written permission.

7/25/68

STRENGTHENING OF TITANIUM CARBIDE BY SURFACE COATINGS

A THESIS

Presented to
the Faculty of the Graduate Division

by

Michael Edward Arthur

In Partial Fulfillment
of the Requirements for the Degree
Master of Science in Ceramic Engineering

Georgia Institute of Technology

March, 1969

STRENGTHENING OF TITANIUM CARBIDE BY SURFACE COATINGS

Approved: _____

Chairman 1 0

Date approved by Chairman: March 22, 1969

ACKNOWLEDGMENTS

The author wishes to express his thanks to Dr. W. E. Moody, School of Ceramic Engineering, Georgia Institute of Technology, for his assistance and guidance in the course of this investigation.

I also thank Dr. Lane Mitchell and Dr. A. T. Chapman for their cooperation as part of my reading committee and Dr. S. C. Bailey for his assistance with the mechanical evaluation.

I would like to thank Mr. Thomas Mackrovitch for his help in machining much of the equipment for this investigation.

The financial aid of the Georgia Institute of Technology and the United States Army Missile Command is gratefully acknowledged.

TABLE OF CONTENTS

	Page
ACKNOWLEDGMENTS	ii
LIST OF TABLES.	iv
LIST OF ILLUSTRATIONS	v
SUMMARY	vi
Chapter	
I. INTRODUCTION	1
II. REVIEW OF LITERATURE	2
Brittle Materials	
Carbides	
Strengthening by Prestressing	
III. EQUIPMENT AND MATERIALS.	12
X-ray Diffractometer	
Mass Spectrometer	
Induction Furnaces	
Microscope	
Materials	
IV. EXPERIMENTAL PROCEDURE	15
Production of TiC Specimens	
Coatings	
Mechanical Evaluation	
V. DISCUSSION OF RESULTS.	22
Oxide Coatings	
Zirconium Diboride Coating	
Boron Carbide Coatings	
VI. CONCLUSIONS.	36
APPENDIX A.	37
BIBLIOGRAPHY.	43

LIST OF TABLES

Table		Page
1.	Polycrystalline Physical Properties (4) of Materials Used in This Investigation	5
2.	Thermal Expansions of Reactants and Products in Equations (6) and (7)	18
3.	Modulus of Rupture and Elastic Modulus Obtained Experimentally for Various Materials	20
4.	Summary of Data Used for Statistical Analysis of the Modulus of Rupture Data	38

LIST OF ILLUSTRATIONS

Figure		Page
1.	Schematic of Stresses in a Laminated Cylinder.	9
2.	Schematic of Composite Beam.	26
3.	B ₄ C Coating on TiC Showing Good Coating of Corners (50X).	30
4.	Interface of B ₄ C Coating on TiC (250X)	31
5.	Interface of B ₄ C Coating on TiC (500X)	32
6.	Corner of B ₄ C Coating on TiC Showing Reaction Layer (darkfield, 250X).	33
7.	Typical Microstructure of TiC (250X)	34

SUMMARY

The basic purpose of this study was to produce a ceramic body in which there was a residual macrostress acting to strengthen the body. The method chosen was to create a compressive surface layer by means of a differential thermal expansion. Because of its potential usefulness, titanium carbide was used as the base material. A number of titanium carbide standards were produced by pressing at 1055 kg/cm^2 with polyvinyl alcohol and sintering.

The two known oxides, Ta_2O_5 and Nb_2O_5 , which possessed thermal expansions lower than titanium carbide were applied and fired. X-ray diffraction and time of flight mass spectrometry studies of the firing process indicated that these two oxides had completely reacted with the TiC to form TaC or NbC, TiO_2 , and CO_2 . From thermodynamic data, the kinetics observed for these reactions, and available thermal expansion data, there appeared to be no oxides available which could be used as a compressive surface coating for TiC.

Zirconium diboride was investigated as a possible coating. There was no bonding between the TiC and the ZrB_2 coating, and the composites showed no increase in flexural strength.

Boron carbide was applied to the specimens, and flexure tests indicated a significant increase in strength from 460 to 726 kg/cm^2 over the standards. The observed increase in the elastic modulus from 5.40

to $11.3 \times 10^5 \text{ kg/cm}^2$ was in close agreement with the Griffith flaw theory. Ceramographic investigation and x-ray analysis indicated that a reaction layer consisting of TiB_2 , C, TiC , and B_4C had been formed at the interface of the coating and base material. The kinetics of this reaction were such that there was a constructive reaction at the interface with excellent coating adherence. Good adherence was noted on the 0.08 cm radius of the corners after firing at 2000°C for one hour.

CHAPTER I

INTRODUCTION

The high temperature properties of ceramic materials make them desirable as high temperature structural components. However, because of their inherent low mechanical strength, ceramic materials have not been widely used as structural materials. Recently much work has been done in attempting to improve the mechanical properties of ceramic materials, particularly in glasses and in polycrystalline oxide systems. These have been systems which, in general, were useful at temperatures below 1500°C. In many fields, aerospace for example, the need for materials which have useful load-bearing capabilities at ambient temperatures in excess of 2000°C has been clearly demonstrated. The most available materials which have melting points in excess of 2500°C are the carbides, borides, and nitrides, as well as a small number of silicides and oxides. One of the more interesting and promising carbides is titanium carbide, having a melting point of 3140°C and showing an increase in tensile strength from room temperature to about 1100°C. Titanium carbide also has a theoretical density of only 4.92 g/cm³ (as compared with densities in excess of ten for many carbides), which should make it particularly attractive for aerospace applications.

CHAPTER II

REVIEW OF LITERATURE

Brittle Materials

When a solid material is subjected to an increasing stress, the material will ultimately break apart. If the failure occurs before the material deforms to a zero thickness, the failure is termed fracture; and if the failure occurs before any permanent (or plastic) deformation takes place, then the failure is termed brittle fracture. The stress-strain diagram for brittle materials will, in general, appear to be a straight line from zero strain and stress to the ultimate strength of the material.

Rosenthal (1) gives an excellent discussion of brittle fracture strength based on the Griffith theory. It is well known that real solids exhibit strengths far below that which can be calculated by theory; and, in particular, brittle polycrystalline materials exhibit this phenomenon. Griffith proposed that the cause of this phenomenon was due to microcracks in the material and was able to experimentally correlate critical crack length (c) of a material and the stress (σ) needed to make the crack propagate, while other investigators have proposed the concept of crack nucleation by means of dislocation pile up. It is possible for the crack to nucleate at a length over the critical length and propagate spontaneously. One source of cracks is the inter-

action of slip bands, causing a piling up of dislocations and the nucleation of cracks. Another major source of cracks is the difficulty encountered in producing a flaw-free surface. In one recent study, Bickelhaupt, et al. (2) reported an increase in the tensile strength of MgO single crystals from 970 to 1294 kg/cm² by polishing the surface. Polishing was accomplished by using a diamond wheel and then by chemically polishing the specimens in orthophosphoric acid.

The critical length of a crack as proposed by Griffith is the maximum length which can be placed in the center of a large brittle plate without the crack propagating spontaneously. If c_1 and c_2 are two critical crack lengths and σ_1 and σ_2 are the stresses needed to propagate the cracks, then

$$\frac{\sigma_1}{\sigma_2} = \frac{\sqrt{c_2}}{\sqrt{c_1}} \quad (1)$$

Further analysis showed that

$$\sigma \sqrt{c} = \sqrt{4\omega E/\pi} \quad (2)$$

where E = Young's modulus for the material

and ω = specific surface energy.

This theory also helps explain the observed differences between compressive and tensile strengths in brittle materials, such as ceramics. Tensile stresses tend to open up the cracks and expand them to their critical length while compressive stresses tend to close the cracks and prevent them from propagating.

Carbides

Carbides are among the most refractory materials known, with many of them having melting points in excess of 3000°C . There is a great variance in the physical and chemical properties of the carbides; the properties of the materials used in this investigation are shown in Table 1. Most carbides are readily oxidized at high temperatures, but some of them are more resistant to oxidation than carbon, graphite, and some refractory metals. Sheipline and Runck (3) state that "although consideration must be given to the atmosphere in which carbides are employed, their retention of mechanical properties at high temperatures and their high melting points suggest their potential usefulness as high-temperature refractories." The most commonly used carbides are silicon, tungsten, and titanium carbide.

Because of its good mechanical properties to about 1100°C , titanium carbide has been of interest as a potentially useful structural material in the aerospace field. Titanium carbide (3) has a metallic gray color, a density of 4.92 g/cm^3 , and a melting point of 3140°C . It has a face-centered cubic structure of the NaCl type with a lattice parameter of 4.3189 \AA .

Williams and Schoal (5) have reported that single crystals of TiC are completely brittle when deformed in compression or bending at temperatures below 800°C . Failure occurs by cleavage on $\{100\}$ planes initiated at surface or internal defects. At temperatures above 800 - 900°C , plastic deformation takes place on the $\{111\}\langle\bar{1}\bar{1}0\rangle$ system.

Vacancies have been commonly recognized as a cause of hardening

Table 1. Polycrystalline Physical Properties (4) of Materials
Used in This Investigation

	TiC	B ₄ C	ZrB ₂
Melting point (°C)	3140	2450	2990
Density (g/cm ³)	4.92	2.51	6.10
Crystal structure	Cubic	Rhom.	Hex.
Lattice parameter (Å): a c	4.32	5.19	3.17 3.53
Color	Metallic Gray	Black	Black
Coefficient of linear expansion (cm/cm°C) × 10 ⁶	8.0	5.6	6.5
Thermal conductivity cal/sec-cm ² , 20°C	.066	.060	.083
Specific heat (cal/g °C), 20°C	0.13	0.22	0.12
Tensile strength (10 ³ kg/cm ²), 20°C 1000°C	1.8 3.0	3.0 1.5	2.0 1.1
Compressive strength (10 ³ kg/cm ²)	13.3-39.3	29.1	15.5
Oxidation resistance in air	51 mg/hr (1000 hrs @ 1000°C)	10 mg/cm ² - hr (1100°C)	4 mg/cm ² (200 hrs @ 1150°C)

in crystal lattices. For example, non-stoichiometric titania (6,7) is stronger than the stoichiometric composition, because of the interactions between dislocations and vacancies or clustered vacancies. In TiC, however, the decrease in strength as the concentration of vacancies increases is attributed to a decrease in the contribution made by carbon atoms in TiC. The nature of the electronic interaction between constituent atoms in the lattice has been deduced from studies of the band structure of the material.

The mechanical properties of the carbides are primarily dependent on at least three variables: stoichiometry, purity, and temperature. There are also three additional variables which also affect the mechanical properties perhaps to a somewhat lesser extent. They are crystal structure, porosity, and grain size. The crystal structure needs more explanation than the remainder of the factors which are common to other compounds. Taylor (8) has shown that, for a polycrystalline aggregate to deform, five independent slip systems are necessary. Groves and Kelly (9) have pointed out that most ceramic materials do not meet these requirements. In the cubic oxide ceramics, for example MgO, slip takes place on $\{110\}\langle\bar{1}\bar{1}0\rangle$ systems. The number of independent slip systems is two and ductility is not shown in polycrystalline material until slip is activated on additional systems. Since the cubic carbides have the five independent slip systems, they are expected to be ductile in polycrystalline form at temperatures not far above the brittle-to-ductile transition temperature found in single crystals although the grain boundaries could be weak due to the atomic mismatch in these di-

rectionally bonded materials. Hexagonal carbides are likely to possess more limited ductility.

Strengthening by Prestressing

It is well known that ceramic materials possess excellent properties at high temperatures with respect to compressive strength, resistance to oxidation, and melting point. However, they have a tensile strength which is usually only about one tenth that of their compressive strength. For this reason, ceramic materials are not commonly used in tensile load-bearing structural applications. One possible method of overcoming this problem is to place a residual compressive macrostress in the material so that, when tension is applied, the compressive forces must first be overcome before the material will fail in tension. This is usually termed prestressing.

There have been a number of methods developed which attempt to place this residual compressive stress in a material. One such method (10) is to quench certain glasses. This method has as its principal limitation the thermal shock resistance of the material. Raju, et al. (11) have developed a method in which ceramic plates were biaxially prestressed to improve their resistance to thermal stress. Greszczuk and Legget (12) have developed a method where tungsten cables are put into tension and zirconia was cast around the cables. The entire system was then heated with the cables still in tension, and the zirconia was sintered at a low temperature to avoid relieving the tension in the cables. When the tension was released, a compressive macrostress was

produced in the zirconia. Kirchner, et al. (13) have done extensive work with the chemical strengthening of ceramic materials in which ions or compounds are added at the surface. Macro stresses were introduced due to differences in thermal expansion between the surface and the center. Chemical strengthening methods (14) have been widely applied in glass.

Kirchner, et al. (13) have listed several mechanisms which have been thought to have contributed to observed increases in strength:

- (1) Low-expansion solid solution surface layers formed by chemical reaction at high temperatures. During cooling after reaction, the main body tends to contract more than the surface layer placing the surface in compression.
- (2) Low-expansion surface layers of a new phase formed by chemical reaction at high temperatures.
- (3) Phase transformations to form less dense phases in the surfaces.
- (4) "Stuffing," that is, exchanging larger atoms for smaller ones in the surface at low temperatures.
- (5) Chemical reactions to form less dense phases in the surfaces.
- (6) Quenching to form a rigid surface layer that is later compressed by the thermal contraction of the underlying material.

The method of producing a compressive surface layer on the material seems to be the most promising, especially in consideration of formation processes. Expansion coefficient differences of only 5×10^{-7} cm/cm°C are sufficient to cause useful compressive stresses in a wide range of sample configurations and body compositions.

Duke, et al. (15) have developed a method for calculating the magnitude of the stress in a composite material with a glaze-type surface coating which is under a compressive load. A diagram of the composite is shown in Figure 1. At the maturation temperature, the surface stress

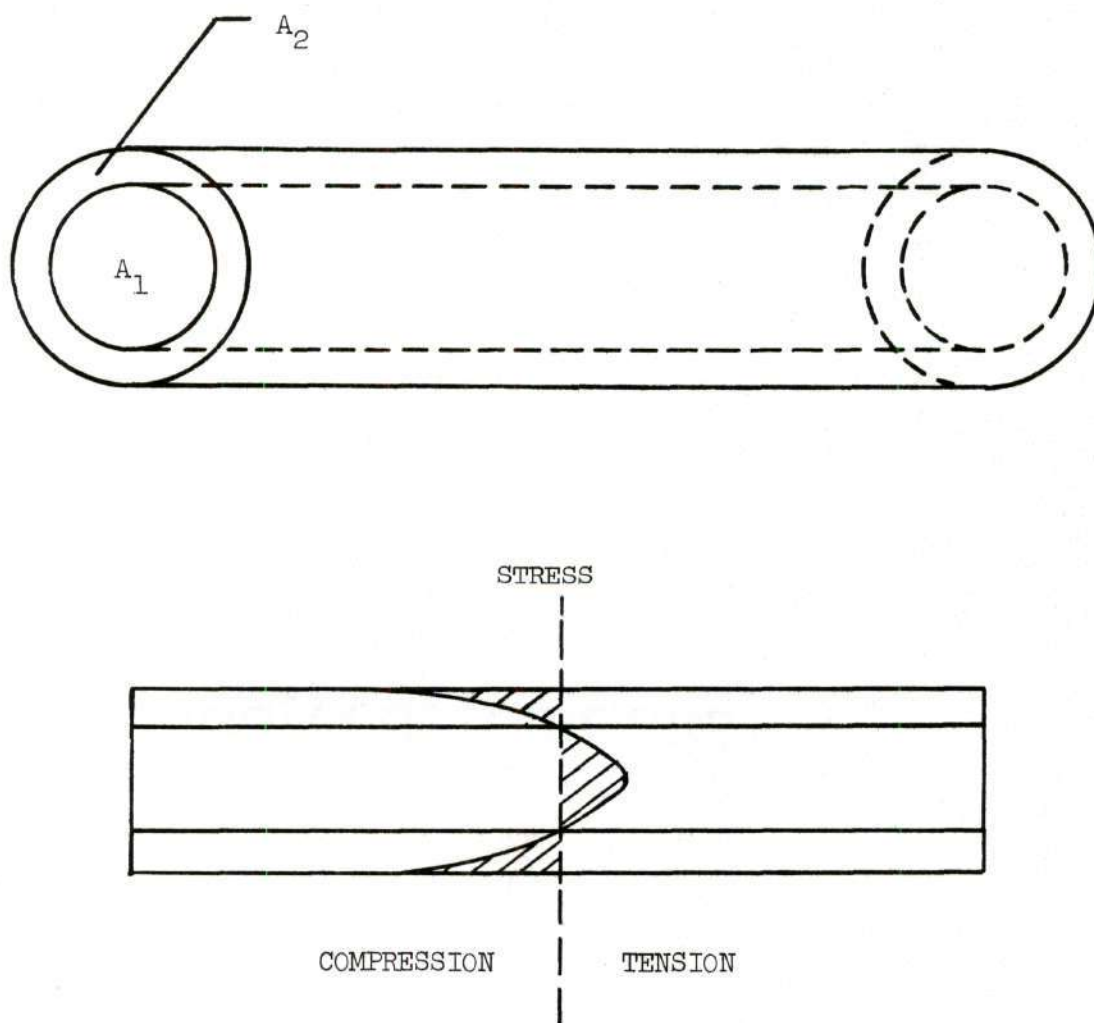


Figure 1. Schematic of Stresses in a Laminated Cylinder

is zero and remains there until the system begins to cool. As this system cools, the effects of the different expansion characteristics are seen. The higher-expansion body continues to contract, and the compressive stress which is induced in the glaze is compensated by an equal tensile force in the body. Four assumptions are made for the formulae:

1. both the surface layer and the body are isotropic and elastic,
2. the temperature distribution is uniform,
3. the elastic moduli and Poisson's ratios are the same for the surface and the body,
4. the radial and circumferential stresses are negligible with respect to the axial stresses.

Then

$$\sigma_s = - (\alpha_1 - \alpha_2) \Delta T \frac{E}{1-\nu} \frac{A_1}{A} \quad (3)$$

and

$$\sigma_b = (\alpha_1 - \alpha_2) \Delta T \frac{E}{1-\nu} \frac{A_2}{A} \quad (4)$$

where

α_1 and α_2 = linear expansion coefficients for the body and glaze, respectively

ΔT = temperature difference between the setting point of the glaze and the temperature where the stress is measured

E = Young's modulus

ν = Poisson's ratio

A_1, A_2, A = cross sectional areas of the body, glaze, and cylinder, respectively

In their studies of titania-nucleated nepheline and nepheline-celsian glass-ceramic with various glazes, good agreement was reported between the calculations made with equations (3) and (4) and the experimental data. Other than the available information on strain and annealing points for some glasses, there are very few reliable data concerning temperature at which a macrostress can be supported in a material. This might make the ΔT term questionable, which would make the calculated stress rather uncertain.

CHAPTER III

EQUIPMENT AND MATERIALS

X-ray Diffractometer

A Norelco diffractometer was used in conjunction with a copper x-ray source which was operated at 40 kv and 25 ma. A nickle filter, a sealed proportional counter, and the associated pulse height analyzer were manufactured by Phillips Electronics, Inc.

Mass Spectrometer

A Bendix Time of Flight Mass Spectrometer was used to ascertain the presence of evolving gases from reactions. The reactants were heated in a high vacuum and the gases were then ionized by electron bombardment. The charged ions were then accelerated by means of an electric field and electron focusing devices. The time taken to travel a specified distance is a function of the ion's mass and charge. The flight tube was 170 cm in length and the information was recorded on a Honeywell Visicorder.

Induction Furnaces

The power was supplied by an Ajax Magnathermic 20 kHz, 6 kw induction furnace of the sealed gap type. The induction coils were water-cooled and were of various sizes supplied by the manufacturer. All the TiC bars were initially sintered in graphite boats in a hori-

zontal Vycor tube furnace with an argon atmosphere. Graphite wool was used for an insulator. Final sintering of the TiC standards was accomplished using a vertical Vycor tube type furnace and by coupling directly to the specimens. They were supported on a small piece of refractory brick and insulated using carbon black. The coated specimens and controls were fired in a horizontal tube furnace consisting of a 3.2 cm diameter graphite tube, a 7.5 cm alumina tube, and a layer of castable refractory between the graphite and the alumina.

Temperature measurements were obtained by means of an optical pyrometer where possible. The graphite tube furnace temperature was measured using the melting points of various refractory metals. Small quantities of nickel (M.P. 1435°C), chromium (M.P. 1550°C), titanium (M.P. 1690°C), vanadium (M.P. 1935°C), and boron (M.P. 2300°C) were placed on a small sheet of tantalum (M.P. 2996°C). After the first runs of the furnace, the nickel and chromium were eliminated.

Microscope

For the ceramographic investigation of the B_4C coatings, a Reichert MeF Research Model microscope was used. The reflected light optics have capabilities to 1200X brightfield and 650X darkfield. Photomicrographs were taken on 10 cm x 12.8 cm plates using Polaroid Type 55P/N, Kodak Contrast Process Ortho, and Kodak Tri-X Pan Professional Film, with the latter being the most prevalent. Development of the negatives and associated prints was carried out using standard procedures.

Materials

Titanium carbide: TAM, Niagara Falls, N. Y., lot 160, -325 mesh.

Tantalum and niobium metal: source unknown.

Zirconium diboride: Cerac, Milwaukee, Wisc., lot IPB-25-13047-64,
-200 mesh.

Boron carbide: Cerac, Milwaukee, Wisc., lot IPB-25-13072-64, -200
mesh.

Carbopol 934: B. F. Goodrich, Cleveland, Ohio, lot 46521.

CHAPTER IV

EXPERIMENTAL PROCEDURE

Production of TiC Specimens

Titanium carbide was chosen as a base material primarily because of two factors: (1) the material has an inherent high strength relative to other carbides and (2) the density is considerably lower than that of most other carbides.

A number of different formation methods were investigated before a suitable process was established. Slip casting was initially used because of the high length-to-diameter ratio desired for mechanical testing. A method developed by Rempes, et al. (16) was used in which the TiC was suspended in a Carbopol (acrylic acid polymer)-sodium alginate aqueous solution. The initial solution consisted of 40 ml of 0.5 percent sodium alginate solution, 20 ml of one percent Carbopol 934, and 100 g of TiC. This produced a slip which contained 62 percent solids. It was very difficult to prevent the formation of hollow, rather than solid, rods even though the plaster molds were vibrated during casting. This slip was varied by eliminating the sodium alginate and varying the solid content from 62 to 20 percent. The Carbopol solution was also changed to a one percent solution in methanol and the solid content varied, but these methods also led to the same results. All suspensions were stable over a period of at least several days.

Extrusion was evaluated using three weight percent Carbopol 934 as a plasticizer as suggested by Hyde (17), but the material tended to pack rather than flow through the die. The die had a 50 degree entrance angle with respect to the direction of material flow.

Another process evaluated was a combination of methods. A graphite mold was machined which was 11.5 cm long and had seven 0.95 cm diameter holes through the length of the mold. The TiC powder was poured into the holes and compacted at a pressure of about 35 kg/cm². The entire mold was then placed in a vertical tube furnace and heated by induction methods in an argon atmosphere to 2200°C for three hours. There appeared to be very little if any reaction between the graphite and the TiC. The strength of specimens produced by this method was somewhat low.

The method finally chosen was a pressing-sintering method. The TiC powder was mixed with one percent polyvinyl alcohol and then compacted in a rectangular 0.64 cm x 0.64 cm x 10.1 cm die at 1055 kg/cm². The bars were then placed in a graphite boat, dried, and sintered at 1000°C for two hours in argon. The standard bars were next placed in an induction furnace and coupled-to directly while packed in carbon black. They were sintered at 2000°C for one hour in argon.

Coatings

Since the coating for TiC was to be placed in compression by means of differential thermal expansion, it was necessary to find a coating which would (1) have a lower thermal expansion than TiC, (2)

be compatible with TiC, i.e., would not react to form other compounds, although a slight reaction at the interface might be desirable, and (3) would bond tightly to the TiC. Other factors which might influence the choice of a coating might be the improvement of oxidation resistance or thermal shock resistance.

In consideration of oxidation resistance, the oxides were reviewed to compare their thermal expansions with that of TiC. Only two, Nb_2O_5 and Ta_2O_5 , were found to have thermal expansions lower than TiC. The thermal expansion of these materials is shown in Table 2.

A small quantity of Ta_2O_5 was prepared by heating tantalum metal powder in air at 1000°C for one hour. The oxide powder was then examined using x-ray diffraction. No evidence was found that would indicate the presence of either unoxidized metal or lower oxides. A suspension consisting of 50 percent solids in a one percent aqueous solution of Carbopol 934 was produced, and the TiC specimens which had been fired to 1000°C were dip coated with the oxide. They were then dried and fired at 1200°C for 30 minutes. A change in color of the fired specimens indicated that the two materials had reacted, and x-ray analysis was employed to ascertain the nature of the reaction.

Niobium oxide was prepared in a manner similar to the Ta_2O_5 , and the material was also applied to the TiC specimens in the same manner. A reaction between the base material and the coating was again indicated by a change in color, and the reaction was investigated using x-ray diffraction and time of flight mass spectrometry.

Two non-oxide coatings were investigated, zirconium diboride and

Table 2. Thermal Expansions of Reactants and Products in Equations (6) and (7)

Material	$\alpha \times 10^6$ (cm/cm °C)
TiC	8.0
Ta ₂ O ₅	1.0
TiO ₂	15.0
TaC	8.2
Nb ₂ O ₅	1.5
NbC	7.6

Note: Values are average expansion values from 0-1000°C.

boron carbide. Both of these were commercially produced and were analyzed by x-ray diffraction to determine if any other phases were present. A suspension consisting of 50 weight percent solids in a one percent solution of Carbopol 934 was applied by dip coating to the TiC specimens which had been fired to 1000°C. After drying, they were fired at 2000°C for one hour along with the controls which had also been fired to only 1000°C previously. Some B₄C coated and dried bars were given an additional coating of B₄C before firing. These were dried again and fired as were the regular coated bars. The B₄C coatings were investigated using ceramographic techniques and x-ray diffraction. The B₄C coated TiC bars were mounted in plastic and were polished for ceramographic investigation using diamond lapping wheels and a Syntron automatic polisher with levigated alumina for final polishing. To determine the presence of any interfacial reaction, small quantities of boron carbide and titanium carbide were reacted in a graphite tube furnace, duplicating the firing conditions of the coated specimens; and the products were analyzed using x-ray diffraction.

Mechanical Evaluation

Both the B₄C and the ZrB₂ coated TiC bars as well as the TiC standards and controls were failed in flexure using three-point loading on a 2.5 cm span; the results are shown in Table 3. A Dillon Model L Universal Testing Machine was used which had a crosshead speed of 0.5 cm/min and a loading rate of 45 kg/min. The B₄C coated TiC and the standards were tested to determine the elastic modulus. This was accom-

Table 3. Modulus of Rupture and Elastic Modulus Obtained Experimentally for Various Materials and Composites

Specimen	MOR (kg/cm ²)	E x 10 ⁻⁵ (kg/cm ²)
TiC standards	460	5.4
TiC controls (average)	420	
ZrB ₂ coated TiC	511	
0.025 cm B ₄ C coating on TiC	726	11.3
0.050 cm B ₄ C coating on TiC	686	
B ₄ C standards	3	

plished by modifying the flexure apparatus to accommodate a dial type deflectometer, which could be read to approximately ± 0.0008 cm. The mechanical design of the fixture kept the knife edge, specimen, and deflectometer in proper alignment with respect to each other. The apparatus was placed in an Instron Universal Testing Machine and a known load applied. Since the beam was supported on two pins at either extreme and loaded in the center, it behaved as a simply supported beam and the elastic modulus of the beam could be calculated as

$$E = \frac{Pl^3}{48I\delta} \quad (5)$$

where

E = elastic modulus of the beam

P = applied load

l = length of the beam between the pin supports

I = moment of inertia around the neutral axis

δ = deflection of the beam in the center

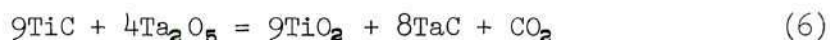
The results of these calculations are shown in Table 3. A statistical analysis (Appendix A) was performed on the data to determine the significance of the data.

CHAPTER V

DISCUSSION OF RESULTS

Oxide Coatings

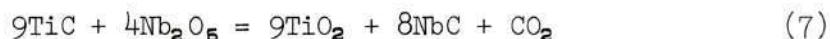
After the Ta_2O_5 coated TiC specimens were fired in argon at $1200^\circ C$ for only 30 minutes, visual examination indicated that some reaction had occurred. This was indicated by the Ta_2O_5 turning from white to a metallic golden color, characteristic of TaC. To ascertain the nature of this reaction, a small quantity of TiC was mixed with Ta_2O_5 and reacted under the same conditions as the specimens. The resultant powder was then examined using x-ray diffraction which indicated the presence of TaC and TiO_2 . These products would suggest a reaction of the form



This was confirmed when the reaction was carried out at $1000^\circ C$ in a time of flight mass spectrometer. This showed that CO_2 was evolved from the reaction. This fact, in conjunction with the x-ray diffraction data, ascertained that all products in equation (6) were present. The change in Gibb's free energy for this reaction at $1200^\circ K$ is -60 kcal (18), thus indicating that the conditions are thermodynamically favorable. The kinetics of the reaction are not known but are apparently quite favorable also, as indicated by the short reaction time involved.

The thermal expansions of the various reactants and products are shown in Table 2. The thermal expansion of neither TaC nor TiO_2 would be suitable for producing a compressive stress in a coating. This would indicate that a coating produced by Ta_2O_5 would not be suitable for a prestressed coating of this nature.

The procedure for applying the coating of Nb_2O_5 to the TiC specimens was identical to the Ta_2O_5 . A lavender color, characteristic of NbC, was observed on the fired specimens in contrast to the usual metallic gray color characteristic of TiC. The reaction was carried out and the products were analyzed by x-ray diffraction. Time of flight mass spectrometry was employed to observe the evolution of CO_2 from the reaction. All reactions were carried out at 1000°C . It is believed that the form of the reaction was



This reaction has a ΔG at 1200°K (18) of -337 kcal which would indicate that the reaction is thermodynamically feasible. The TiO_2 formed will in this case also prevent the formation of any useful compressive stresses in the surface layer. From thermodynamic data, the kinetics of these reactions, and available thermal expansion data, there appeared to be no suitable oxide coating that could be used as a compressive surface coating for TiC.

Zirconium Diboride Coatings

Zirconium diboride was evaluated as a possible coating for TiC. The modulus of rupture for ZrB_2 coated TiC specimens was 511 kg/cm^2 , which was slightly higher than the standards and controls but could not be termed significantly higher than the standards as is shown in Appendix A. Visual examination of the coated specimens indicated that there was no bonding of any magnitude between the body and the coating. It was felt that there was neither any mechanical adherence, even though the surface of the TiC was fairly rough, nor any chemical bonding between the TiC and the ZrB_2 . Although no thermodynamic data were obtainable for ZrB_2 , this would seem to indicate that the TiC and ZrB_2 are more stable at this temperature (1000°C) than the TiB_2 and ZrC which might be formed in a chemical reaction between the body and the coating.

Boron Carbide Coatings

Boron carbide was chosen because of its thermal expansion and outstanding physical properties. A number of B_4C coated TiC rods were prepared and tested in flexure. The modulus of rupture was found to be 726 kg/cm^2 , as compared with 460 kg/cm^2 for the standards. It may be shown (Appendix A) that this can be said to be a significant increase (as opposed to experimental error) with a certainty of 99.95 percent.

It may be easily shown that the strength of the composite beams produced was not simply the sum of the two materials. The extreme stress (19) in any fiber is given by

$$s = \frac{Mc}{I} \quad (8)$$

where

s = unit stress on any fiber, usually that most distant from the neutral surface

c = distance of that fiber from the neutral surface

M = bending moment = force \times distance

I = moment of inertia of the cross section with respect to its neutral axis

A rectangular composite of the type investigated here is shown schematically in Figure 2. The subscript 1 refers to the coating, while 2 refers to the body. The maximum stress in a simply supported beam loaded in the center may be calculated from equation (8). The stress in the coating is

$$s_1 = \frac{M_1 c_1}{I_1} \quad (9)$$

where

s_1 = stress in the coating

$$M_1 = \frac{w_1 \ell}{4}$$

$$c_1 = \frac{d_1}{2}$$

$$I_1 = \frac{b_1 d_1^3 - b_2 d_2^3}{12}$$

w_1 = applied load

The maximum stress in the base may be calculated from

$$s_2 = \frac{M_2 c_2}{I_2} \quad (10)$$

where

s_2 = stress in base

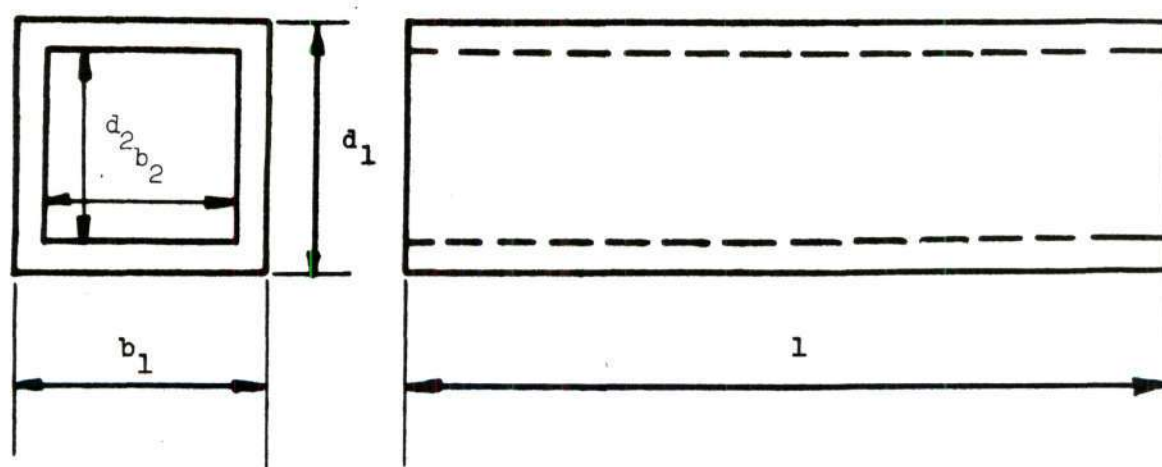


Figure 2. Schematic of Composite Beam

$$M_2 = \frac{w_2 \ell}{4}$$

$$c_2 = \frac{d_2}{4}$$

$$I_2 = \frac{b_2 d_2^3}{12}$$

w_2 = applied load

Then the breaking load may be found to be

$$w_1 = 2s_1 \frac{(b_1 d_1^3 - b_2 d_2^3)}{3\ell d_1} \quad (11)$$

and

$$w_2 = \frac{2s_2 b_2 d_2^2}{3\ell} \quad (12)$$

Thus, if the dimensions and the values of s_1 and s_2 (determined experimentally) are known, w_1 and w_2 may be calculated. These are the breaking loads if no prestressing exists. The breaking load by superposition should be simply

$$w_{\text{total}} = w_1 + w_2 \quad (13)$$

However, if a compressive stress is induced into the outer shell, then

$$w_{\text{total}} > w_1 + w_2 \quad (14)$$

The flexure equation (8) holds only for those stresses in the proportional limits of the material but not at the breaking load. Therefore, the actual breaking stress cannot be calculated. If the compressive and tensile strengths are different (as are most ceramic

materials), then the modulus of rupture is an intermediate value between the two. It is, however, very useful as a basis of comparison, especially when identical conditions (such as span, loading rate, and head speed) are present.

Consider a bar of TiC, 0.635 cm x 0.635 cm, with a uniform coating of B_4C 0.0076 cm thick. If each of the beams is considered to be independently broken, the breaking load of the base material was found to be 30.9 kg, based on experimental data and a 2.5 cm span as calculated from equation (12). From equation (11), the breaking load of the coating would be 0.0024 kg. Therefore, the total breaking load would be approximately 30.9 kg. The low value determined for the s_1 used for the B_4C was believed to be due to the processing. Even if this value were increased by three orders of magnitude, the breaking load of the coating would be 2.4 kg, and the composite should break at 33.4 kg. However, using the actual experimental value for the s of the composite, the breaking load would be calculated to be 50.6 kg. This is an increase of 63 percent over the value obtained if no prestressing were present and strengths were simply additive.

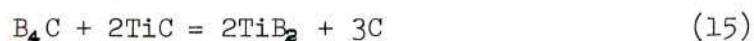
As was indicated in equation (2), the strength of a brittle material (such as TiC) is directly proportional to the square root of the elastic modulus of the material. The increase in elastic modulus from 5.40 to 11.3×10^5 kg/cm² was indicative of an increase in strength of the material. The square root of the ratio of the elastic moduli of the two materials was 1.50 which meant that the strength of the composite might be predicted to be 1.50 that of the standards. The actual

ratio, determined experimentally, was 1.58, which was well within experimental error.

Examination of these coatings revealed the adherence to be extremely good. This was true even for the corners (which had been slightly rounded from a right angle to a radius of about 0.08 cm) as shown in Figure 3. This radius may be favorably compared to a minimum radius of about 0.6 cm for porcelain enamel (typically fired to only 800°C for five minutes), whereas the B₄C coating was fired to 2000°C for one hour.

Ceramographic examination of the coating showed that net adherence was produced by a combination of mechanical and chemical adherence. The mechanical contribution is shown in Figure 4 where the roughness of the interface between the coating and the body may be seen. This may be seen at higher magnification in Figure 5.

Examination of the interface suggested that a reaction layer might have been formed. This is believed to be the light area at the interface as shown in Figure 6. Glaser (20) suggests the reaction



will occur at the relatively low temperature of 1200°C when the materials are hot-pressed. To confirm this, a small quantity of the two materials was heated to 2000°C and held there for one hour, duplicating the firing cycle given the coatings on the TiC rods. The presence of TiB₂ was confirmed by x-ray diffraction. Ceramographic examination also verified that a reaction layer was present.

The thickness of the coating was optically measured to be 0.027 cm.

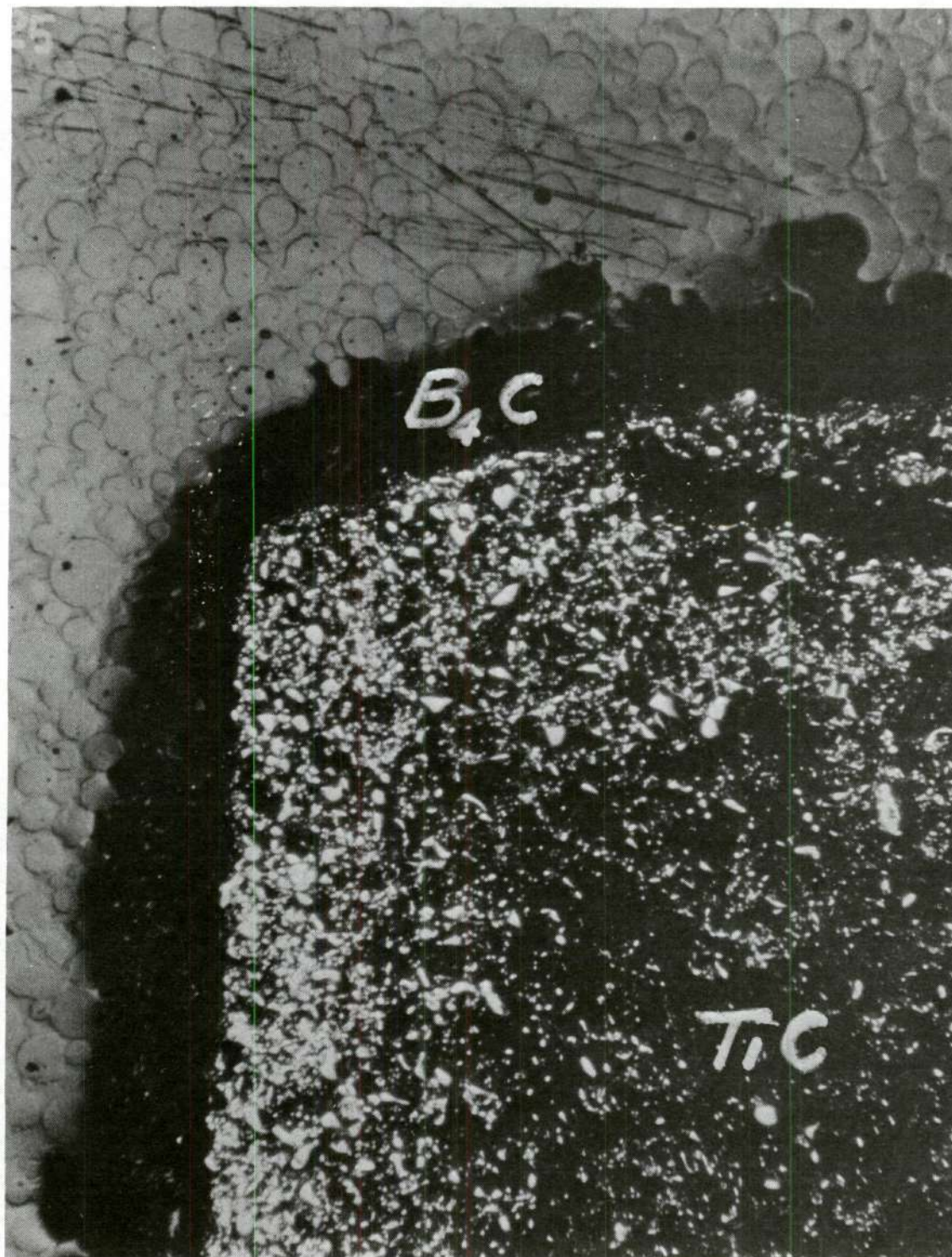


Figure 3. B_4C Coating on TiC Showing Good Coating of Corners (50X)

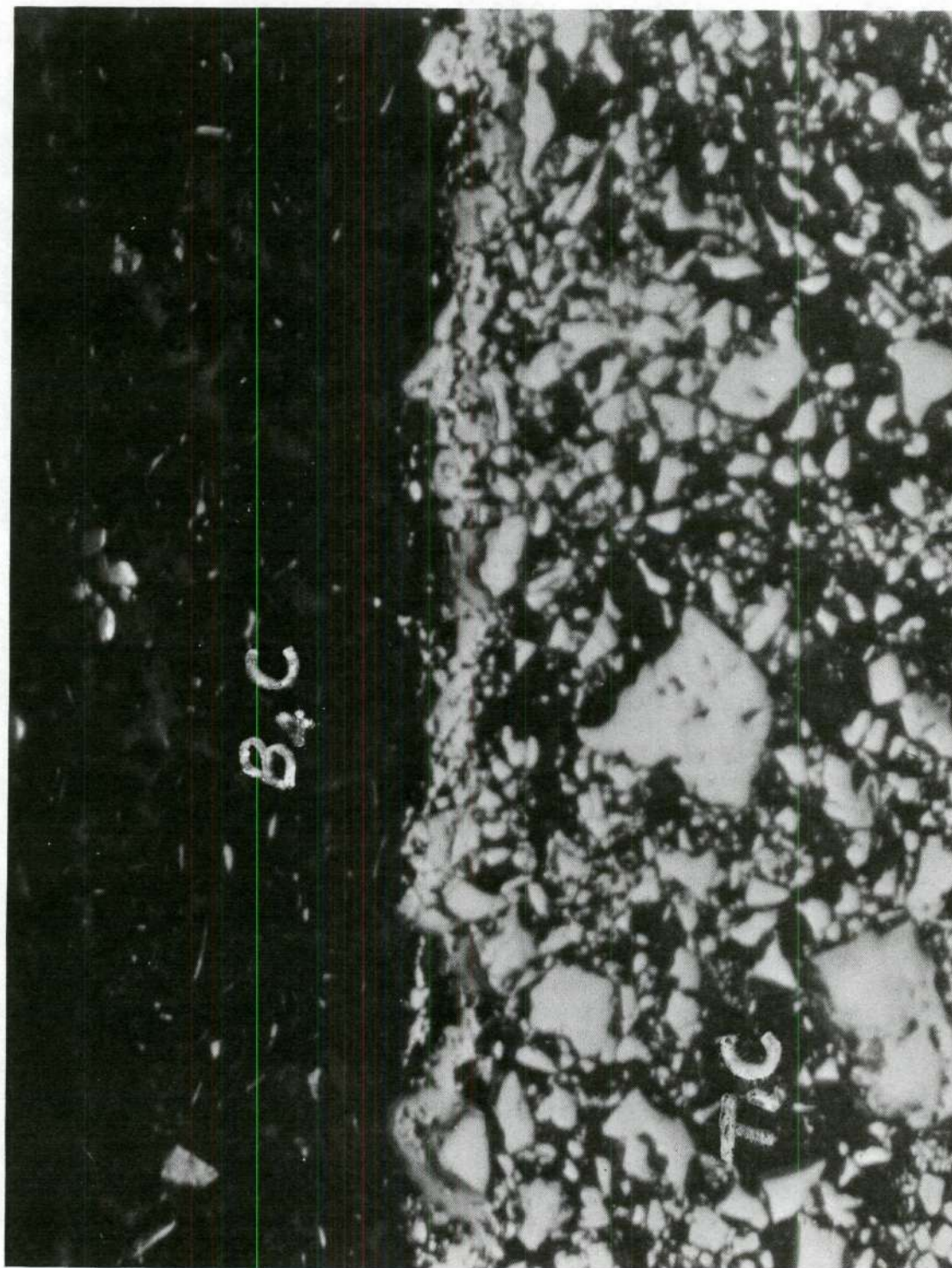


Figure 4. Interface of B₄C Coating on TiC (250X).

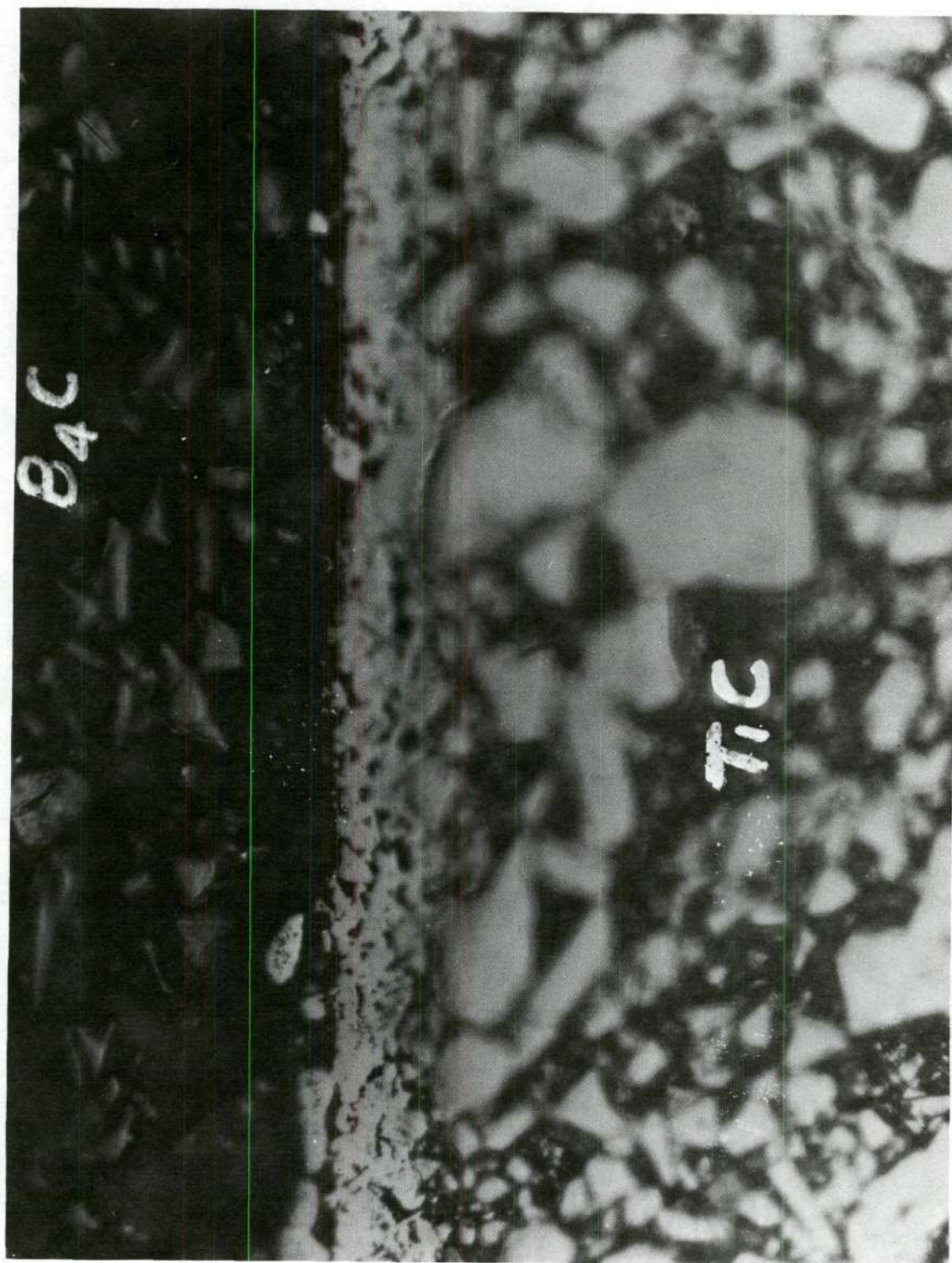


Figure 5. Interface of B₄C Coating on TiC (500X).

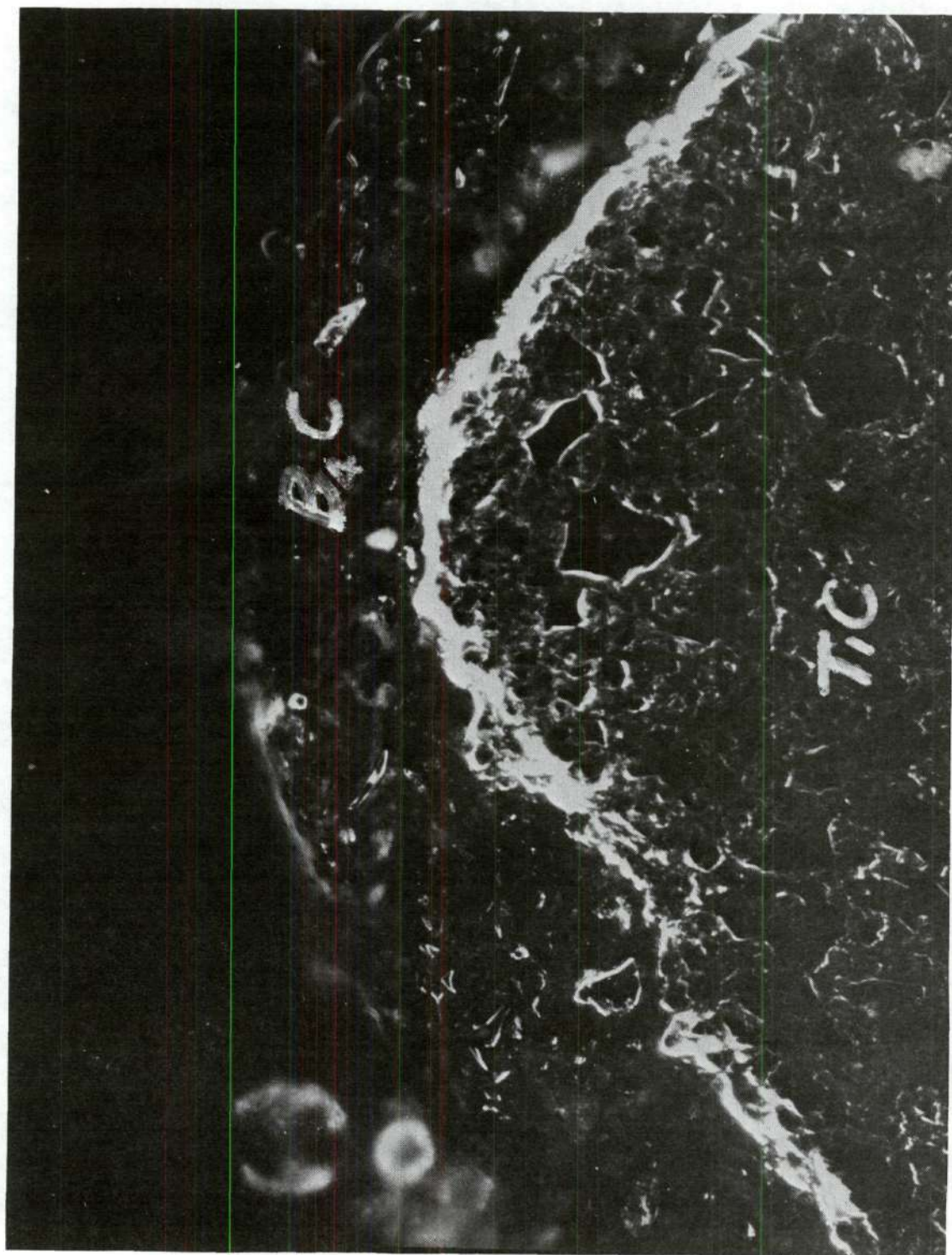


Figure 6. Corner of B₄C Showing Reaction Layer (darkfield, 250X).



Figure 7. Typical Microstructure of TiC (250X).

There was some pull back and burnoff on the corners reducing the thickness to about 0.015 cm. The double-coated bars possessed a coating thickness of 0.051 cm and a modulus of rupture of 686 kg/cm^2 , which could not be shown to be significantly different from the single-coated bars (Appendix A). This evidence would indicate that coatings of B_4C 0.027 cm on TiC would significantly increase the strength of TiC.

CHAPTER VI

CONCLUSIONS

1. A 0.025 cm coating of B_4C on 0.625 cm square cross sectional TiC bars will significantly increase the flexural strength of TiC. The strengthening and good adherence are due to a combination of the mechanical adherence and chemical reaction to form $TiB_2 + C$ at the interface.
2. Due to its lack of good adherence, ZrB_2 will not significantly strengthen TiC.
3. A reaction to form TaC, TiO_2 , and CO_2 causes Ta_2O_5 to be unsuitable as a prestressed coating for TiC.
4. A reaction to form NbC, TiO_2 , and CO_2 causes Nb_2O_5 to be unsuitable as a prestressed coating for TiC.

APPENDIX A

STATISTICAL ANALYSIS OF DATA

In this section it is assumed that (1) all variables are normally distributed and (2) the variables have equal variances. The latter statement may easily be verified by means of F ratio tests and will be proved for each pair of standard deviations. The data used for this analysis are given in Table 4.

Table 4. Summary of Data Used for Statistical Analysis of the Modulus of Rupture Data

Specimen	i	\bar{x}_i^*	n_i^*	s_i^*
TiC standards	1	460	17	163
TiC controls	2	420	8	114
ZrB ₂ coated TiC	3	511	9	101
0.025 cm B ₄ C coating on TiC	4	726	21	94
0.050 cm B ₄ C coating on TiC	5	686	5	148
B ₄ C standards	6	3.0	4	1.3

* In this table, the subscript "i" indicates the number used in the analysis, \bar{x}_i is the average value, n_i is the number of samples of a given specimen, and s_i is the standard deviation.

I) Comparison of TiC controls with TiC standards.

$$H_0: \sigma_1^2 = \sigma_2^2$$

$$H_a: \sigma_1^2 \neq \sigma_2^2$$

$$\text{Accept if } \frac{s_1^2}{s_2^2} < F_{.01}(16, 7) = 6.27$$

Reject otherwise.

$$\frac{(163)^2}{(114)^2} = 2.06 < 6.27$$

$$\text{Conclude } \sigma_1^2 = \sigma_2^2$$

$$H_0: \mu_1 = \mu_2$$

$$H_a: \mu_1 \neq \mu_2$$

Accept if

$$|\bar{x}_1 - \bar{x}_2| < t_{(1-\alpha/2, v)} \sqrt{\frac{(n_1-1)s_1^2 + (n_2-1)s_2^2}{n_1+n_2-2}} \sqrt{\frac{n_1+n_2}{n_1n_2}}$$

$$\text{Let } \alpha = .01$$

$$v = n_1 + n_2 - 2 = 23$$

$$|460 - 420| < 2.807 \sqrt{\frac{16(163)^2 + 7(114)^2}{17+8-2}} \sqrt{\frac{17+8}{17 \cdot 8}}$$

$$40 < 180$$

Conclude there is no difference in MOR between standards and controls.

II) Comparison of ZrB_2 coated TiC with TiC standards.

$$H_0: \sigma_1^2 = \sigma_3^2$$

$$H_a: \sigma_1^2 \neq \sigma_3^2$$

$$\text{Accept if } \frac{s_1^2}{s_3^2} < F_{.01}(16, 8) = 5.48$$

Conclude that the TiC standards and the ZrB_2 coated specimens have equal variances.

$$H_0: \mu_3 > \mu_1$$

$$H_a: \mu_3 \leq \mu_1$$

Accept if

$$\bar{x}_3 - \bar{x}_1 > t_{(1-\alpha/2, \nu)} \sqrt{\frac{(n_1-1)s_1^2 + (n_3-1)s_3^2}{n_1+n_3-2}} \sqrt{\frac{n_1+n_3}{n_1n_3}}$$

$$\text{Let } \alpha = .005$$

$$\nu = n_1 + n_3 - 2 = 24$$

$$511 - 460 > 2.797 \sqrt{\frac{16(163)^2 + 8(101)^2}{17+9-2}} \sqrt{\frac{17+9}{17 \cdot 9}}$$

$$51 < 174$$

Reject H_0 , conclude there is no difference at this level of significance in MOR between the TiC standards and ZrB_2 coated TiC.

III) Comparison of 0.025 cm B₄C coated TiC specimens with TiC standards.

$$H_0: \sigma_1^2 = \sigma_4^2$$

$$H_a: \sigma_1^2 \neq \sigma_4^2$$

$$\text{Accept if } \frac{s_1^2}{s_4^2} < F_{.01}(16, 20) = 3.05$$

$$\frac{(163)^2}{(94)^2} + 3.00 < 3.05$$

Conclude that the variables have equal variances.

$$H_0: \mu_4 > \mu_1$$

$$H_a: \mu_4 \leq \mu_1$$

$$\text{Let } \alpha = .0005, \quad v = n_1 + n_2 - 2 = 36$$

Accept if

$$\bar{x}_4 - \bar{x}_1 > t_{(1-\alpha/2, v)} \sqrt{\frac{(n_1-1)s_1^2 + (n_4-1)s_4^2}{n_1+n_4-2}} \sqrt{\frac{n_1+n_4}{n_1n_4}}$$

$$726 - 460 > 3.608 \sqrt{\frac{16(163)^2 + (20)(94)^2}{17+21-2}} \sqrt{\frac{17+21}{17 \cdot 21}}$$

$$226 > 152$$

Conclude that there is a significant increase in the strengths of the 0.025 cm B₄C coated TiC over the TiC standards at the 0.05 percent level.

IV) Comparison of the 0.025 cm B₄C with the 0.050 B₄C coated TiC.

$$H_0: \sigma_4^2 = \sigma_5^2$$

$$H_a: \sigma_4^2 \neq \sigma_5^2$$

$$\text{Accept if } \frac{s_5^2}{s_4^2} < F_{.01}(4, 20) = 4.43$$

$$\frac{(148)^2}{(94)^2} = 2.26 < 4.43$$

Conclude the two variables have equal variances.

$$H_0: \mu_4 = \mu_5$$

$$H_a: \mu_4 \neq \mu_5$$

Accept if

$$|x_4 - x_5| < t_{(1-\alpha/2, \nu)} \sqrt{\frac{(n_4-1)s_4^2 + (n_5-1)s_5^2}{n_4+n_5-2}} \sqrt{\frac{n_4+n_5}{n_4n_5}}$$

$$\text{Let } \alpha = .01$$

$$\nu = n_4 + n_5 - 2 = 24$$

$$40 < 2.797 \sqrt{\frac{20(94)^2 + 4(148)^2}{21+5-2}} \sqrt{\frac{21+5}{21 \cdot 5}}$$

$$40 < 146$$

Conclude that the increase in B₄C coating thickness from 0.025 to 0.050 cm does not affect the MOR.

BIBLIOGRAPHY

1. Rosenthal, Daniel, "Introduction to Properties of Materials," pp. 123-27, D. van Nostrand Co., Inc., Princeton, N. J., 1964.
2. Bickelhaupt, et al., "Diffusional Prestressing of Ceramics," Summary Report Nr. 8504-1780-XV, July 6, 1967, Southern Research Institute, Birmingham, Ala.
3. Sheipline, V. M. and Runck, R. J., "Carbides," being Chapter 5 pp. 114-30 "High Temperature Technology" edited by Campbell, I. E., John Wiley and Sons, Inc., New York, 1956.
4. "Refractory Ceramics for Aerospace," compiled by Battelle Memorial Institute, Columbus, Ohio, published by the American Ceramic Society, Inc., Columbus, Ohio, 1964.
5. Williams, W. S. and Schaal, R. D., "Elastic Deformation, Plastic Flow, and Dislocations in Single Crystals of Titanium Carbide," J. App. Phy., 33, 955-62 (March 1962).
6. Ashbee, K. H. G. and Smallman, R. E., "Plastic Deformation of Titania Single Crystals," Proc. Royal Soc. London, A274, 195 (July 1963).
7. Hollox, G. E. and Smallman, R. E., "The Effect of Stoichiometry on the Yield Stress of TiC and TiO₂," Proc. Brit. Cer. Soc., 6, 317 (1966).
8. Taylor, G. I., "The Mechanism of Plastic Deformation of Crystals. Pt. I--Theoretical," Proc. Royal Soc. London, A145, 362 (July 1934).
9. Groves, G. W. and Kelly, A., "Slip Systems in Crystals," Phil. Mag., 8, 877 (May 1963).
10. Fletcher, Peter C. and Tilman, J. J., "Effect of Silicone Quenching and Acid Polishing on the Strength of Glass," J. Am. Cer. Soc., 47, 379-82 (August 1968).